Dynamic Light Scattering; a Method to Determine Thermal Diffusivity and Thermal Conductivity of Environmentally Acceptable Refrigerants

B. Kruppa, J. Straub

Lehrstuhl A für Thermodynamik, Technische Universität München, P.O. Box 202420, 80333 München 2, Federal Republic of Germany

ABSTRACT

Dynamic light scattering is an efficient method for determining the thermal diffusivity and thermal conductivity of transparent fluids in a wide region of state. Its main advantage in comparison with conventional methods is that measurements are conducted under thermodynamic equilibrium. The transport properties are derived by investigating the temporal behaviour of microscopic fluctuations in the thermodynamic variables.

This paper presents our thermal diffusivity measurements of the environmentally acceptable refrigerants R22, R134a and R123, the last two substances being possible substitutes for the refrigerants R12 and R11 respectively. Measurements were performed along the critical isochore, both coexisting phases and up to seven isotherms. In the extended critical region (characterized in terms of reduced density as $0.3 < \varrho/\varrho_c < 1.8$) the homodyne technique of light scattering was employed. The application of the heterodyne technique has enabled us to extend the investigated range of state into the fluid region ($\varrho/\varrho_c < 2.5$) as well as improve the quality of the measurements in the gas region ($\varrho/\varrho_c > 0.2$). Simple correlation equations are given which enable the thermal diffusivity to be calculated to within 10% in the entire investigated region. Provided with an equation of state to determine c_p, the diffusivity data can also be expressed in terms of thermal conductivity λ. This is particularly useful in the critical region where the conventional hot-wire and parallel plates techniques are particularly subject to error.

1. INTRODUCTION

A knowledge of the thermodynamic properties of working fluids in processes operating under thermodynamic cycles is necessary, not only for a better understanding of the process itself, but also for planning and designing the appropriate components. With low and mediate temperature cyclic processes such as refrigeration processes, there is still a lack of thermophysical data of the appropriate working fluids, particularly in the area of transport properties. This is due to the fact that transport properties such as thermal conductivity, diffusivity and viscosity are generally difficult to measure and are burdened with uncertainties typically an order of magnitude greater than their corresponding equilibrium properties (such as p, ϱ,T -measurements).

This is shown quite clearly in the current search for environmentally acceptable substitutes for the chlorofluorocarbons typically used in these processes, which are responsible for the depletion of the stratospheric ozone layer. While, after more than 5 years of research, the equilibrium p,ϱ,T -properties of the most promising alternatives CH_2FCF_3 (R134a) and $CHCl_2CF_3$ (R123) have been investigated sufficiently to allow for the development of tables and equations, the amount of reliable measurement data on transport properties is far less and not nearly as evenly distributed, with some regions of state totally lacking measurements.

For calculations involving heat transfer, it is the knowledge of the transport properties that constitutes a necessary information for designing and dimensioning components, the properties appearing often in the dimensionless numbers as Nusselt, Reynolds, Prandtl, Grashof and Rayleigh.

In this paper, our thermal diffusivity measurements of the alternative refrigerants R22, R134a and R123 obtained by light scattering are presented. With a good equation of state for ϱ and c_p, thermal conductivity can be calculated from the diffusivity data as will be shown for the substance R22. Our measurements also cover the critical region, where conventional stationary and instationary methods for determining λ are subject to large errors due to convective effects and are hence particularly scarce. Here, dynamic light scattering can also be used as an accurate method to determine λ.

2. METHOD OF MEASUREMENT

Dynamic light scattering represents a non-invasive optical technique for measuring thermal diffusivity. The fluid under investigation is kept in thermal equilibrium with no internal sources of heat or macroscopic temperature gradients present, which is a significant advantage over the conventional techniques of determining transport properties such as the parallel plate or hot wire methods. The information on thermal diffusivity is obtained by investigating the relaxation behaviour of microscopic thermodynamic fluctuations. Since the method is intrinsically absolute in nature, there is no need for calibration or for introducing corrective terms. According to the optical arrangement for detecting the scattered light, measurements can be made in the fluid region (heterodyne detection) and in the extended critical region (homodyne detection) with an accuracy typically under 2% depending on the investigated region of state. At lower fluid densities (below 100 kg/m^3) the scattered intensities are too low to be evaluated accurately, and thus limit the range of application. For an explicit treatment of dynamic light scattering and its applications we refer to the standard literature [1] − [3].

The experimental apparatus used in our investigations has been described in detail by [4] − [6]. An argon-ion laser with a maximum power output of 300 mW is focussed into a test cell. The light scattered by the microscopic temperature fluctuations is recorded at variable scattering angles (3° − 15°) by a photomultiplier. This signal is then fed into a digital correlator which builds the correlation function g(t), the statistical average behaviour of the dissipative fluctuations. A regressional analysis yields the characteristic decay-time t_c of this exponential function from which thermal diffusivity can directly be calculated.

On account of the relatively high critical temperatures of the alternative refrigerants, we have developed an electronically regulated test cell capable of sustaining a long term temperature stability (± 2 mK over 24 h) at temperatures up to 500 K [7]. This stability is important when measuring in the critical region where the thermal diffusivity a decreases over several orders of magnitude and where macroscopic temperature stability not only limits the possible approach to the critical point but also represents an increasing source of error in the determination of a. In this investigation we have been able to measure thermal diffusivites to within 0.01 K of the critical point. While the above-mentioned temperature stability would allow for closer approaches, other limiting factors such as multiple scattering, gravitation, laser heating or limits of the hydrodynamic region become a major source of error in this region.

In the extended critical region, measurements were made using the homodyne method of light scattering. The scattered light $\bar{I}_S$ is directly measured by the photomultiplier at angles Θ between $8° - 10°$. Light scattered off the cell windous I_0 (representing a local oscillator) is effectively screened out of the detection by means of a pinhole situated in front of the cell windows, ensuring the criterion $\bar{I}_S \gg I_0$ for the evaluation of the correlation function by a single exponental.

In the fluid region, where scattered light intensities are small, the heterodyne method was employed. Here signal enhancement is achieved by superimposing a local oscillator, the light I_0 scattered off the cell windows, with $\bar{I}_S$. By measuring at small scattering angles (Θ between $3° - 5°$) and shifting the scattering volume with respect to the window surface, the assumption $I_0 \gg \bar{I}_S$ can be assured.

3. RESULTS

The objective behind this investigation was a systematic coverage of a broad region of state within the limits set by the applicability of the method or the apparatus. For this reason, thermal diffusivity measurements were made along four super- and up to three subcritical isotherms $\tau = \pm 10^{-3}, \pm 10^{-2}, \pm 5 \cdot 10^{-2}$ and $+10^{-1}$, where τ denotes the reduced temperature and is characterized by $\tau = (T - T_c)/T_c$. Measurements were also made along the critical isochore as well as both coexisting phases. On average, 35 measurement points were taken along each path. The covered region of state expressed in terms of density and pressure is approximately $100 \text{ kg/m}^3 < \rho < 1200 \text{ kg/m}^3$ and $290 \text{ K} < T < 420 \text{ K}$. While the measurements at higher temperatures and pressures were restricted by the pressure resistance of the quartz cell windows, those obtained in the low density region were limited by the applicability of the method due to low light scattering intensities.

In addition to thermal diffusivity, the temperature, pressure and refractive index of the substances were also measured. Using the Lorentz - Lorenz relation, density values can be calculated from the refractive index measurements.

Figures 1 to 5 depict the measured values of thermal diffusivity of the substances R22, R134a and R123. Figures 1 and 3 plot a against the reduced temperature in double logarithmic axes for both phases of the coexistence curve and for the critical isochore. The logarithmic presentations in Figures 2 and 4 depict a vs. the reduced density ϱ/ϱ_c for the coexistence curve and seven isotherms. Figure 5 shows the thermal
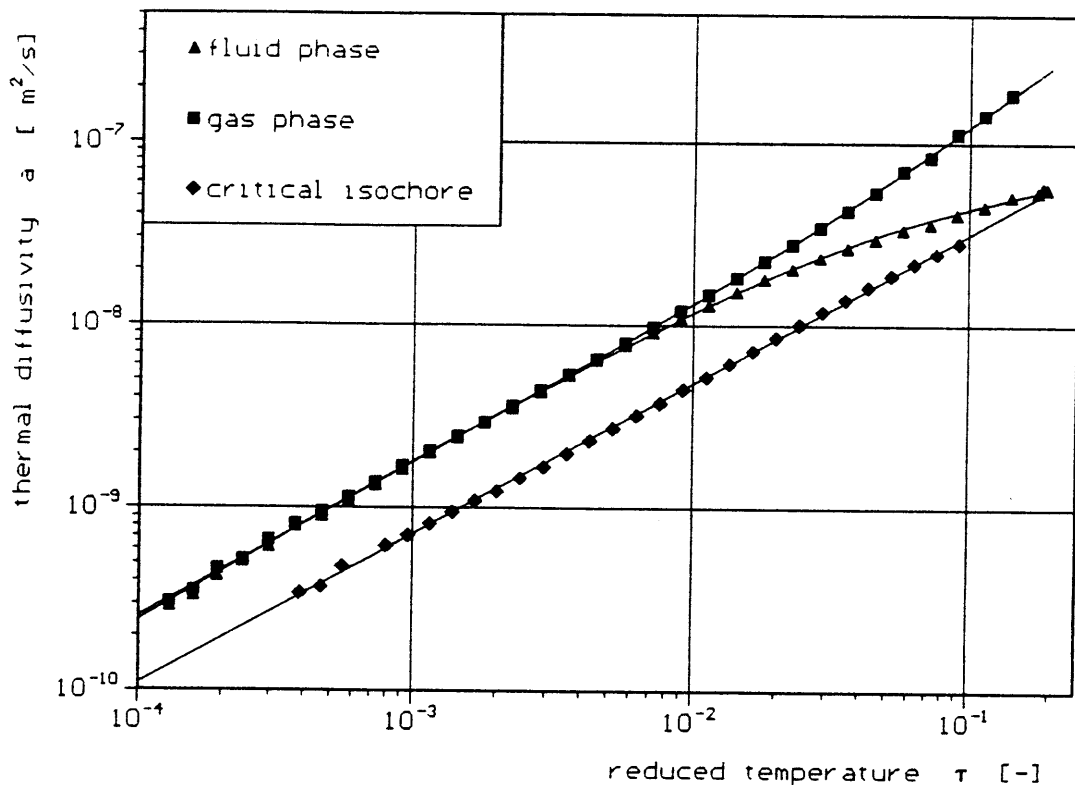
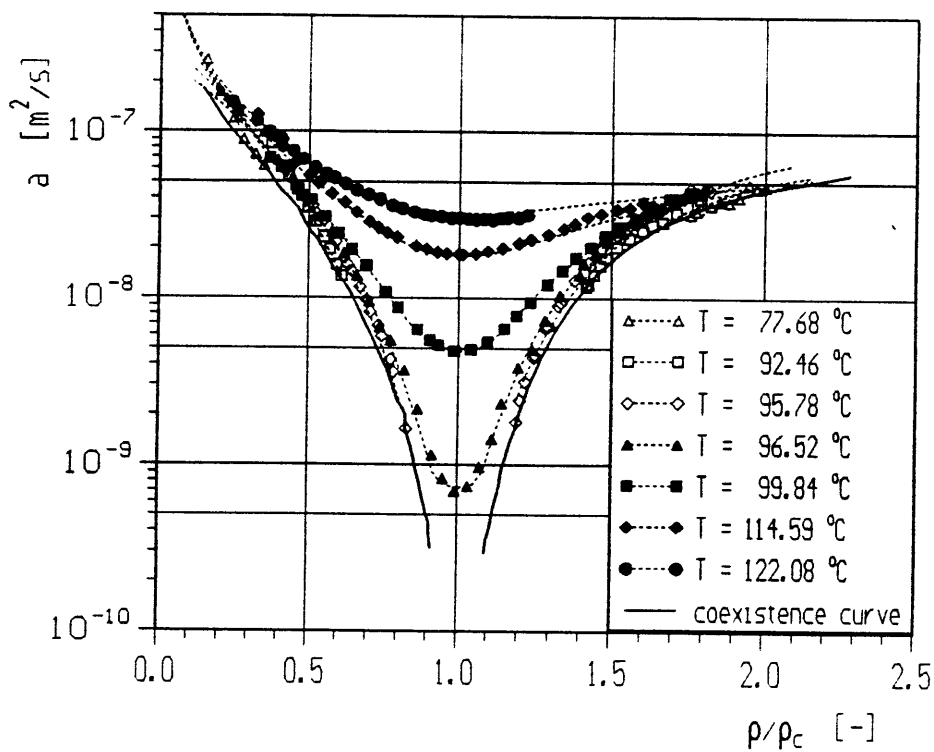Fig.1 Thermal diffusivity of R22 along the two-phase region and critical isochore

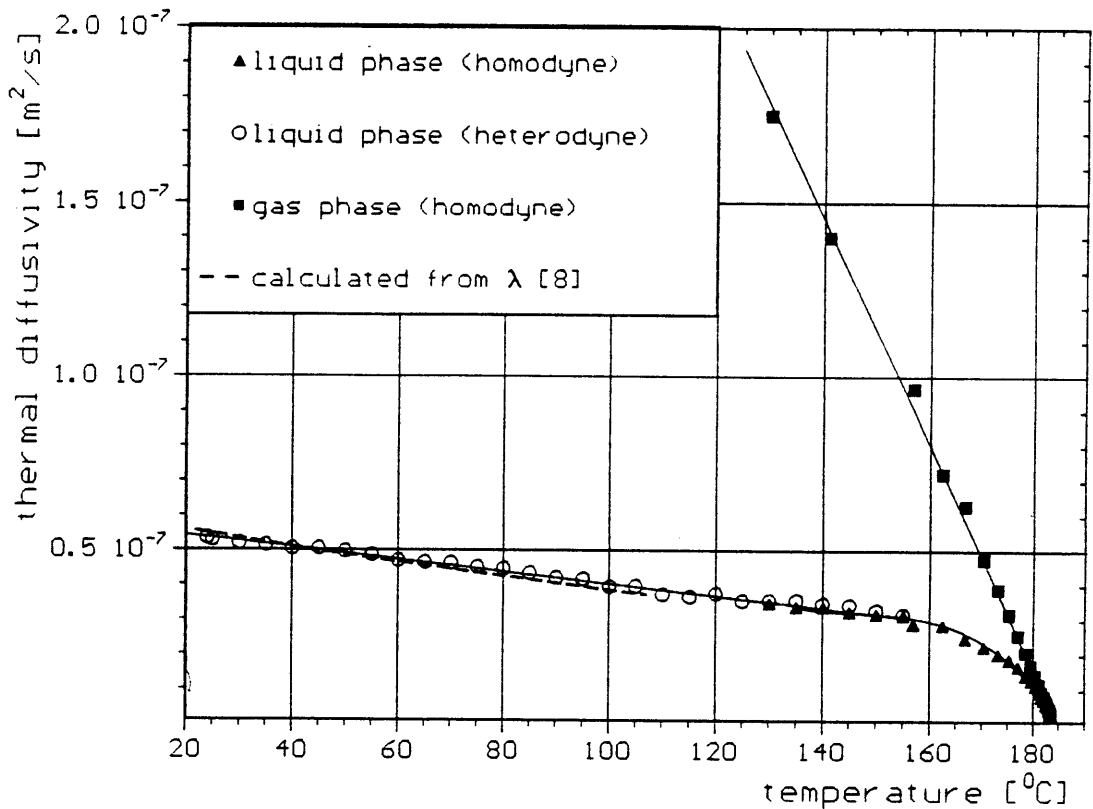Fig.2 Thermal diffusivity of R22 along isotherms

Fig.5 Thermal diffusivity of R123 along the two-phase region

diffusivity of the refrigerant R123 along both phses of the coexistence
cure plotted linearly against the Temperature T. In the liquid phase, at
temperatures below $155°C$, we applied the heterodyne technique, while
the other regions were investigated with the homodyne technique of
light scattering. The region of overlap $130°C \leq T \leq 155°C$ shows good
agreement between the two methods. A comparison with converted
thermal conductivity measurements in the fluid region [8] also shows
good agreement. As can be seen from the figure, the combination of
the two techniques allows for a wide range of states to be investigated.
Since the refrigerant R123 dissociated in our apparatus near the critical
point ($\sim 183°C$) no isotherms could be investigated.

4. ACCURACIES

4.1 Thermal diffusivity

Since dynamic light scattering represents a statistical process, the
measurements of diffusivities are invariably subject to statistical devia-
tion in addition to experimental errors. In the following we will briefly
classify the main sources of error. The equation determining thermal

diffusivity, obtained from [1 − 3], can be expressed as:

$$\mathbf{a} = \frac{1}{t_c \, \vec{q}^{\,2}} \tag{1}$$

where $\vec{q}$ is the scattering vector and defines the scattering geometry

$$|\vec{q}| = q = \frac{4\pi n}{\lambda_L} sin\left(\frac{\Theta}{2}\right). \tag{2}$$

Here n is the refractive index of the fluid, λ_L the wavelength of the incident light and Θ the scattering angle. Errors made in the determination of $\vec{q}$ can easily be assesed.

λ_L - The error in the wavelength of the incident light can be neglected, as the use of a frequency stabilizing etalon reduces this error to the order of $10^{-3}\%$.

n - Aside from its direct influence on **a**, refractive index errors also affect the determination of the scattering angle Θ due to the optical geometry. However, both errors have a compensating effect, such that a deviation $\Delta n/n$ of 10% only contributes to an error in $\Delta \mathbf{a}/\mathbf{a}$ of 0.3% [6]. Thus n-measurements need not necessarily be made. In our experiments the refractive index is determined with an accuracy of $\Delta n < 5 \cdot 10^{-4}$. The resulting error of Δn on $\Delta \mathbf{a}/\mathbf{a}$ is of the order 0.08%.

Θ - The scattering angle must be carefully measured. In our apparatus, Θ is measured with an accuracy $\Delta \Theta < 6$" using a high precision dividing head. Thus, its overall effect on $\Delta \mathbf{a}/\mathbf{a} < 0.05\%$ is relatively small.

t_c - The main source of error lies in the determination of the decay time t_c through digital correlation due to the statistical process involved. A detailed treatment of the statistical accuracy in light scattering experiments, including such error sources as afterpulse and dead-time effects of the detection system, bias, optimizing experimental parameters (such as photon counts/sampletime, sampletime/decaytime, runtime ect.) can be found in [9 − 10].

Perhaps the single largest error in light scattering experiments arises from an undesired influence of both measurement methods known as partial heterodyning or homodyning. If the afore-mentioned assumptions $\bar{I}_S \gg I_0$ or $I_0 \gg \bar{I}_S$ are not satisfied in homodyne or heterodyne experiments respectively, the correlation function, which is fitted to a

single exponential is contaminated by the addition of a second exponential, the decay times differing by a factor 2. An I_0 contribution of 0.5% in homodyne experiments can already account for errors in the determination of **a** of the order of 1% [11]. $\overline{I}_S/I_0$ can be estimated from the correlated data, or obtained directly by experiment (evacuating the test cell keeping all other parameters constant). In homodyne experiments, this source of error becomes noticeable at further distances from the critical point, where low light scattering signals and a corresponding high laser power increases the contribution of I_0. We have been able to keep the influence of this error source on **a** under 1% in most cases.

In the immediate critical region the geometry of the test cell and that of the optical setup increasingly influences the accuracy of diffusivity measurements. Gravitation, multiple scattering, limits of the hydrodynamic region and laser heating are the main sources of error and have been treated in [7].

The overall accuracy of our thermal diffusivity measurements lies between 0.5 - 5%, those obtained in the critical region being more accurate than measurements made in regions of low light scattering intensities.

p,ϱ,T - Data

T - The fluid temperature was measured with a low-drift platinum resistance thermometer (PT 100) with a resolution under 1mK. Calibration resulted in a maximum absolute temperature deviation of 20mK between 50 - 150 $^\circ C$. A repeated measurement of the critical temperature of R22 within two years revealed negligible drift.

p - A piezoresistive pressure transducer was used for measurements. Here calibration over 15 MPa resulted in a maximum deviation of $5 \cdot 10^{-3}$ MPa while the resolution was under $1 \cdot 10^{-4}$ MPa.

ϱ - Density was calculated from the refractive index data using the Lorentz-Lorenz relation. With $\Delta n = 5 \cdot 10^{-4}$, the resulting accuracy in the density measurements is 0.3%. A comparison of our measured R22 densities with an accurate equation of state [12] yields maximum deviations of 0.7%.

5. EVALUATION

5.1 Critical values

Measurements made along the coexistence curve and the critical isochore closely approach the critical point, enabling the determination of

critical parameters. Critical temperature T_c is determined by an optical method and by the evaluation of the refractive index data, the latter method being the more precise. The refractive index measurements also yield values for n_c and, assuming ϱ_c from the literature, the Lorentz-Lorenz constant LL_c. Table 1 lists the critical values for the substances R22, R134a and R123.

Table 1

Critical values

	T_c [K]	n_c [−]	p_c [MPa]	ϱ_c [kgm^{-3}]	LL_c [m^{3}kmol^{-1}]
R22	369.29	1.1109	4.965	520.0 [12]	11.846
R134a	374.09	1.0885	4.030	512.2 [13]	11.561
R123	457.37	1.1207	3.650	555 [8]	21.610

While the T_c and p_c values for R22 are in good agreement with those of other authors [14], the values for R134a and R123 differ from those reported by [13, 8, 15 and 16].

5.2 Thermal diffusivity

The thermal diffusivity data obtained along the coexistence curve and the critical isochore, when plotted in double logarithmic form along reduced temperature, appears as a straight line in the critical region and can be described by a simple power law which is also in accordance with scaling theory

$$\mathbf{a} = a_0 \tau^\mu. \tag{3}$$

This equation can be used to describe thermal diffusivity along the critical isochore (ci) in the entire investigated region. However, in the fluid and gas phases, the measurements deviate off the straight line at further distances from the critical point. As expected, the fluid phase levels out to a linear behaviour while measurements along the gas phase

increase, reflecting ideal gas behaviour. With the addition of a temperature dependent term in the exponent, this behaviour can be accounted for

$$\mathbf{a} = a_0 \mid \tau \mid^{\mu_0 + \mu_1 \mid \tau \mid}. \tag{4}$$

Table 2 lists the coefficients obtained by regressional analysis along the respective paths for the three refrigerants.

Table 2

Coefficients resulting from a fit to Equations 3 and 4

	critical isochore		fluid phase			gas phase		
	a_{ci} $[10^{-7}]$	μ	a_0 $[10^{-7}]$	μ_0	μ_1	a_0 $[10^{-7}]$	μ_0	μ_1
R22	2.101	0.820	8.244	0.885	3.89	5.771	0.838	-1.73
R134a	2.140	0.811	8.904	0.880	4.89	6.231	0.830	-2.71
R123	–	–	9.736	0.898	5.37	11.61	0.921	-0.62

The exponents μ and μ_0 are larger than the theoretical value $\nu = 0.63$ from scaling theory. A regional fit of our data by approaching the critical point shows no indication of these values to decrease. The data can also be fitted by an expansion

$$\mathbf{a} = a_0 \mid \tau \mid^{\mu} (1 + a_1 \tau^{\Delta} + a_2 \tau^{2\Delta} \ldots) \tag{5}$$

in analogy with the *corrections to scaling* [17] taking into account the extended region around the critical point, with Δ being a correction exponent. However, the initial values for μ and Δ have to be kept within strict boundaries close to the expected theoretical values, and standard deviations of the fit double. If the critical exponent is determined according to its original definition

$$\mu = \lim_{\tau \to 0} \frac{d \, ln(\mathbf{a})}{d \, ln(\tau)}, \tag{6}$$

then the values in table 2 are more reliable than the theoretical one.

A simple expression for the thermal diffusivity along isotherms as a function of density is more difficult to establish, due to the large differences encountered when describing the values ranging from the ideal gas region ($a \to \infty$), over the critical point ($a \to 0$) to the fluid region, where a exhibits linear behaviour. An effective method presented here, is to describe the investigated region of state in terms of reduced density σ and reduced temperature τ

$$\tau = \frac{T - T_c}{T_c}, \qquad \sigma = \frac{\varrho_c - \varrho}{\varrho_c}, \tag{7}$$

and by separating the regions into $T > T_c$, $T < T_c$, $\varrho > \varrho_c$ and $\varrho < \varrho_c$. Furthermore, since the thermal diffusivity of different substances along isotherms exhibits a very similar behaviour (Figs. 2 and 4), the measurements can be expressed in reduced form, with the respective values a_{ci}, obtained from the evaluation of the data along the critical isochore (table 2), being a suitable normalisation constant. This results in a set of 4 equations

$$\frac{a(\tau > 0, \sigma < 0)}{a_{0_{ci}}} = a_1 exp(-a_2 \mid \sigma \mid^{-\beta_1}) + \tau^{\mu}$$

$$\frac{a(\tau > 0, \sigma > 0)}{a_{0_{ci}}} = a_3 exp(-a_2 \mid \sigma \mid^{-\beta_1}) + \tau^{\mu} + \frac{a_4 \mid \sigma \mid^3}{(1- \mid \sigma \mid)^{0.6 \mid \sigma \mid}}$$

$$\frac{a(\tau < 0, \sigma < 0)}{a_{0_{ci}}} = a_5 \mid \sigma \mid^{\beta_2(2-\mid\sigma\mid)}$$

$$\frac{a(\tau < 0, \sigma > 0)}{a_{0_{ci}}} = a_6 \mid \sigma \mid^{\beta_3} . \tag{8a-d}$$

The coefficients of the supercritical isotherms $\tau > 0$ can be developed as a function of temperature

$$a_1 = -2.95 - 1.82 \cdot ln(\tau)$$
$$a_2 = 2.5 \cdot \tau^{-0.05}$$
$$\beta_1 = 0.38$$
$$a_3 = 1.78 \cdot \tau^{-0.2}$$
$$a_4 = 0.6, \tag{9a-d}$$

allowing for arbitrary isotherms to be calculated.

Table 3

coefficients of the reduced thermal diffusivity according to equations 8c and 8d along subcritical isotherms.

region		a_6	β_3	a_5	β_2
	$\tau = 10^{-3}$	1.33	2.91		
$\sigma > 0$	$\tau = 10^{-2}$	1.71	3.47		
	$\tau = 5 \cdot 10^{-2}$	2.53	5.25		
	$\tau = 10^{-3}$			0.28	1.06
$\sigma < 0$	$\tau = 10^{-2}$			0.23	0.99
	$\tau = 5 \cdot 10^{-2}$			0.215	1.19

Since the sub-critical isotherms ($\tau < 0$) consist of only relatively few data points, the thermal diffusivity can only be calculated along those isotherms investigated here, the coefficients being listed in table 3.

With the above set of equations, the thermal diffusivity can be calculated to within 10% of the measured data within the entire investigated region.

5.3 Thermal conductivity

Thermal conductivity can be calculated from the diffusivity data using the equation $a = \lambda/\rho c_p$, provided a good equation for the Helmholtz free energy or an equation of state with an appropriate value of c_{p0} is available, allowing for the determination of ρ and c_p from the T,p-data.

Figure 6 shows λ of the refrigerant R22 as calculated from our thermal diffusivity data along 4 supercritical isotherms and the 2 phase region. The values of c_p were obtained by an equation for the free Helmholtz energy developed by [12], while ϱ was calculated from our refractive index measurements. Measurements obtained by Makita [18] with the concentric cylinder apparatus are also included. While the agreement at distances further from the critical point is very good ($100°C$), large differences are observed in the critical region, the values of Makita being larger than those measured by light scattering. This may be due to convective effects in the concentric cylinder apparatus. The new conductivity data of Assael [19] along the saturated fluid phase is in good agreement with our data.
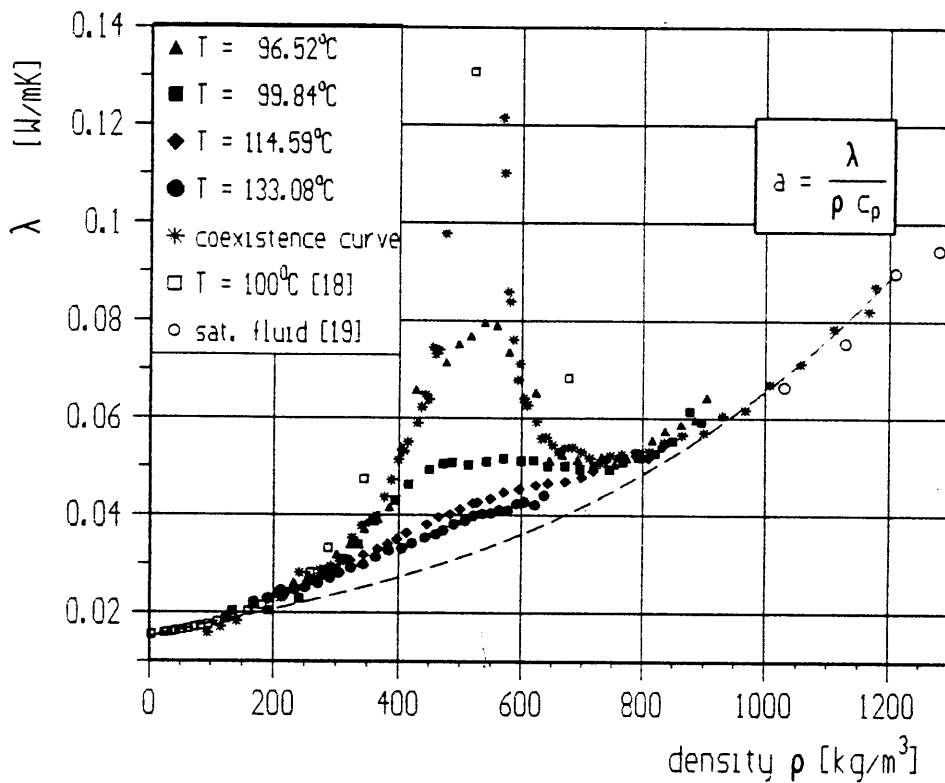
Fig.6 Thermal conductivity of R22

6. CONCLUSIONS

Light scattering measurements of thermal diffusivity of the alternative refrigerants R22, R134a and R123 have been presented, proving this method to be an effective means of measuring this transport property in a broad region of state characterized by 100 kg/m^3 < ϱ < 1200 kg/m^3. By combining the techniques of homodyne and heterodyne detection, measurements can be made up to pressures and temperatures usually limited by constraints imposed by the test cell. In the gas region at lower densities, dynamic light scattering is subject to increasing errors due to low scattering intensites and thus cannot be applied. The accuracy of the light scattering measurements varies between 0.5 and 5.0%, depending on the investigated region of state. The measurements can be described by power laws and simple equations within an error of 10%. Dynamic light scattering can also serve as a complementary technique for determining thermal conductivity, particulary in the critical region, where conventional methods are subject to error. We hope this work serves as a contribution for a better coverage of thermophysical property data of the new environmentally acceptable refrigerants.

ACKNOWLEDGEMENTS

REFERENCES

1 Berne, B.J., Pecora, R., *Dynamic Light Scattering*, John Whiley, New York, 1976.

2 Chu, B., *Laser Light Scattering*, Academic Press, New York, 1974.

3 Pecora, R., *Dynamic Light Scattering, Applications of Photon Correlation Spectroscopy*, Plenum Press, New York, 1985.

4 Reile, E., Jany, P., Straub, J., *Wärme- und Stoffübertragung*, (1984), 18: 99-108.

5 Jany, P., Straub, J., *Int. J. of Thermophys.*, (1987) 8: 165-180.

6 Kruppa, B., Die Temperaturleitfähigkeit alternativer Kältemittel in einem weiten Temperatur- und Dichtebereich, *Ph.D.-Thesis*, (1993), Technical University Munich, FRG.

7 Kruppa, B., Straub, J., *Int. J. of Thermophys.*, (1988), 9: 911-922.

8 Japanese Association of Refrigeration, *Thermophysical Properties of Refrigerants R134a and R123*, Tokyo, 1991.

9 Jakeman, E., Pike, E.R., Swain, S., *J. Phys A: Gen. Phys.*, (1971), 4: 517.

10 Degiorgio, V., Lastovka, L.B., *Phys. Rev. A*, (1971) 4: 2033.

11 Ford, N.C., *Chemica Scripta*, (1972), 2: 193.

12 Marx, V., Pruß, A., Wagner, W., *Fortschritt- Berichte VDI*, VDI-Verlag (eds.), 19:57 (1992).

13 Basu, R.S., Wilson, D.P., *Int. J. of Thermophys.*, (1988) 10: 591-604.

14 Japanese Association of Refrigeration, *Thermophysical Properties of Refrigerants R22*, Tokyo, 1975.

15 McLinden, M.O., Gallagher, J.S., Weber, L.A., *ASHRAE Trans.* (1989), 96.

16 Kubota, H., Yamashita, T., Tanaka, Y., Makita, T., *Int. J. of Thermophs.*, (1989) 10: 629-638.

17 Wegner, F.J., 1972. *Phys. Rev. B*, (1972) 5: 4529-4536.

18 Makita, T., Tanaka, Y., Morimoto, Y., Noguchi, M., Kubota, H., *Int. J. of Thermophys.*, (1981) 2: 249-268.

19 Assael, M.J., Karagiannidis, E., *paper presented at the workshop: Thermophysical Properties of Environmentally Acceptable Refrigerants*, Ericeira, Portugal, Nov. 1992.